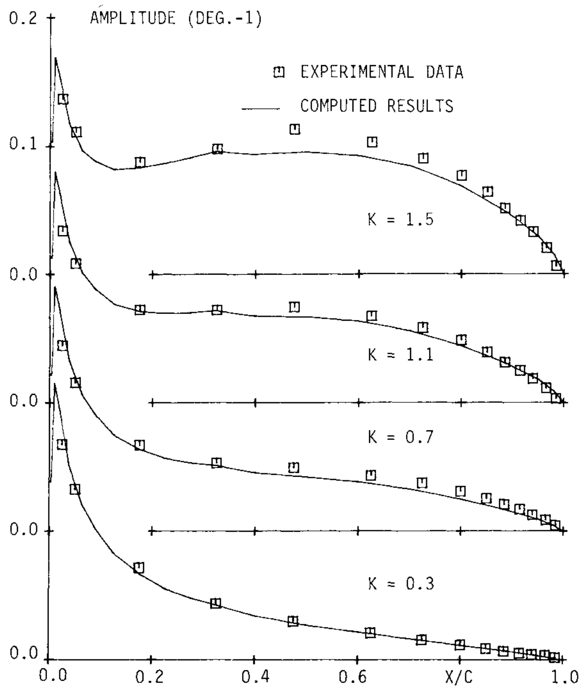

Fig. 2 Comparison between the measured and computed amplitude of the surface-pressure fluctuations. The unsteady pressure coefficient K_p is divided by the amplitude of the angular fluctuation (1 deg).

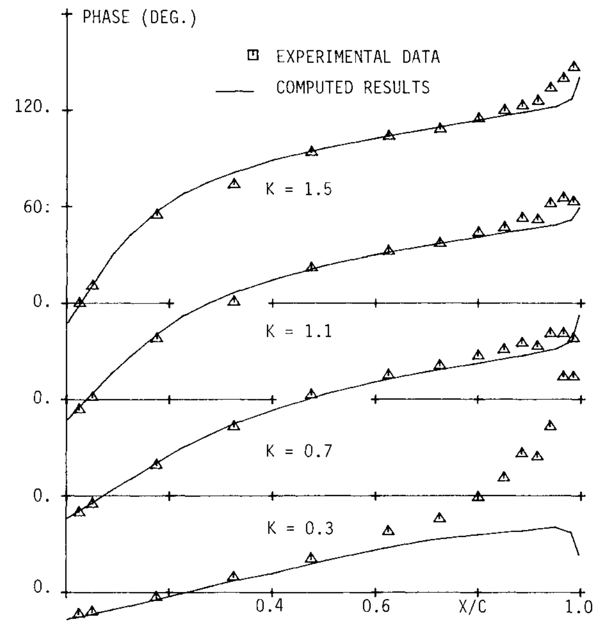

Fig. 3 Comparison between the measured and computed phases of the surface pressure fluctuations.

sured amplitude and phase of the first harmonic of the unsteady pressure are presented in Figs. 2 and 3 for several values of the reduced frequency k.

The general agreement is good, except for the phase in the trailing-edge region at the lower reduced frequency. The experimental determination of the phase seems questionable, since the amplitude is very small and the signal becomes "noisy" due to turbulent fluctuations. Another discrepancy appears at $k = 1.5$ in the amplitude comparison. Here, a bending of the wing occurs due to the high frequency, and a plunging motion is superposed to the pitching motion.

Discussion and Conclusion

The overall agreement between the measured and computed pressure fluctuations over a pitching airfoil seems to validate the inviscid model in a range of reduced frequencies extending up to $k = 1.5$. The predicted loading of the trailing-edge region agrees well with the measured values, and no spectacular deviation appears. The deviation between the theoretical and experimental data mentioned by Ref. 1 has not been verified, either for the amplitude or the phase comparisons. Although the wing section is different (NACA 64A010 in Ref. 1), the others parameters (amplitude, Reynolds number, reduced frequency) are identical.

The question of whether the Kutta condition is verified or not depends on the exact meaning given to this condition. As far as the differential pressure loading in the trailing edge region is concerned, the condition is verified, at least in the range of amplitude and reduced frequencies that were investigated. However, the phenomenological behavior of the velocity as described by Maskell[9] cannot be proven, either experimentally, since the flow is viscous, or numerically, due to the singularity of the solution at the trailing edge in the physical plane.

References

[1]Satyanarayana, B. and Davis, S., "Experimental Studies of Unsteady Trailing Edge Conditions," *AIAA Journal,* Vol. 16, Feb. 1978, pp. 125–129.

[2]Bass, R., Johnson, J., and Unruh, J., "Correlation of Lift and Boundary-Layer Activity on an Oscillating Lifting Surface," *AIAA Journal,* Vol. 20, Aug. 1982, pp. 1051–1056.

[3]McCroskey, W., "Unsteady Airfoils," *Annual Review of Fluid Mechanics,* Vol. 14, 1982, pp. 285–311.

[4]Telionis, D. and Poling, D., "The Response of Airfoils to Periodic Disturbances. The Unsteady Kutta Condition," AIAA Paper 84-0050, 1984.

[5]Schlichting, H. and Truckenbrodt, E., *Aerodynamics of the Airplane,* McGraw-Hill, New York, 1975.

[6]Van Dyke, M., "Perturbation Methods in Fluid Mechanics," *Applied Mathematics and Mechanics,* Vol. 8, 1964, pp. 121–146.

[7]Kaplun, S., *Fluid Mechanics and Singular Perturbations,* Academic Press, New York, 1967.

[8]Ardonceau, P., "La condition de Kutta Joukowski en aérodynamique instationnaire," *Proceedings of the 22nd AAAF Conference,* AAAF, Paris, France, 1985.

[9]Basu, B. and Hancock, G., "The Unsteady Motion of a Two-Dimensional Aerofoil in Incompressible Inviscid Flow," *Journal of Fluid Mechanics,* Vol. 87, Pt. 1, 1978, pp. 159–178.

[10]Sears, W., "Unsteady Motion of Airfoils with Boundary-Layer Separation," *AIAA Journal,* Vol. 14, Feb. 1976, pp. 216–220.

[11]Giesing, J., "Vorticity and Kutta Condition for Unsteady Multi-Energy Flows," *Transactions of the ASME, Journal of Applied Mechanics,* Vol. 36, No. 3, Sept. 1969, pp. 608–613.

[12]Sato, J., "Settling Times of Pressure Measurements through Capillary Tubes," *AIAA Journal,* Vol. 17, Oct. 1979.

Coupled Thermoelasticity Beam Problems

M. R. Eslami* and H. Vahedi†
Tehran Polytechnic, Tehran, Iran

Introduction

RAPID changes in thermal gradient with respect to time of an elastic continuum requires that the first law of thermodynamics include rate effects; therefore, the solution for tem-

Received Dec. 14, 1987; revision received May 23, 1988.

*Associate Professor, Mechanical Engineering Department.
†Graduate Student, Mechanical Engineering Department.

perature distribution requires the simultaneous solution of the thermal and elasticity equations. Nowacki[1] has developed this subject very well. Due to mathematical complexity analytical treatment of such problems is not possible, and thus an efficient, powerful, and general numerical scheme seems essential. Galerkin's method, which has been applied to many engineering problems in recent years, seems quite suitable for treating this class of problems. In that regard, Fletcher[2] has presented recently the general application of the Galerkin method in mathematical problems of mechanics; Eslami and Salehzadeh[3] have used this concept to develop a finite-element scheme to handle coupled thermoelastic problems. This Note represents a continuation of the work in Ref. 3 and presents a general approach for the application of the Galerkin method to coupled thermoelasticity problems.

Governing Equations

The general governing equations of coupled thermoelasticity are[1]

$$\tau_{ij,j} = \ell \ddot{u}_i \tag{1}$$

$$\epsilon_{ij} = \tfrac{1}{2}(u_{i,j} + u_{j,i}) \tag{2}$$

$$\tau_{ij} = 2\mu\epsilon_{ij} + \lambda\epsilon_{kk}\delta_{ij} - (3\lambda + 2\mu)\alpha(T - T_0)\delta_{ij} \tag{3}$$

$$T_{,ii} - \frac{1}{\kappa}\dot{T} - \frac{\alpha T_0(3\lambda + 2\mu)}{k}\dot{\epsilon}_{ii} = -\frac{Q}{k} \tag{4}$$

where σ_{ij} and ϵ_{ij} are the stress and strain tensors, U_i the displacement components, T the absolute temperature, μ and λ the Lamé constants, α the coefficient of thermal expansion, k the thermal conductivity, κ the thermal diffusivity, T_0 the temperature in the unrestrained state, ℓ the mass density, and Q the rate of energy generation per unit volume. When combined, the first three equations yield equilibrium equations in terms of displacement components as

$$\mu\, u_{i,kk} + (\lambda + \mu)u_{k,ki} - (3\lambda + 2\mu)\alpha\, T_{,i} = \ell\, \ddot{u}_i \tag{5}$$

When solved simultaneously, Eqs. (4) and (5) give the general solution for coupled thermoelasticity problems.

Application of the Galerkin Method

The foregoing governing equations do not have a general analytical solution, but a finite-element formulation may be developed based on the Galerkin method. In the following, a generalized procedure is developed that can be applied to this class of problems. The solution domain is discretized and in each element the components of displacement and temperature are approximated by the following functions[4]:

$$u_i = \sum_{m=1}^{n} U_{mi}(t) \cdot \Phi_{mi}(x^s) \tag{6}$$

$$T = \sum_{m=1}^{n} T_m(t) \cdot \Psi_m(x^s) \tag{7}$$

This is a Kantorovich type of approximation, where time and space dependence are separated into distinct functions. $U_{mi}(t)$ is the component of displacement at each nodal point and $T_m(t)$ the temperature at each nodal point. All are functions of time. The variables $\Phi_{mi}(x^s)$ and $\Psi_m(x^s)$ are the shape functions. The number of nodal points in the element is taken as n. Substituting Eqs. (6) and (7) into Eq. (4) and applying the weighted residual method with respect to the weighting functions $\Psi_m(x^s)$, the formal Galerkin approximation reduces to

$$\sum_{m=1}^{n}\int_v \left[T_m\Psi_{m,ii} - \frac{1}{\kappa}\dot{T}_m\Psi_m - \beta\,\dot{U}_{mi}\phi_{mi,i} + \frac{Q}{k}\right]\Psi_l\,\mathrm{d}V = 0$$

$$l = 1,n;\; i = 1,3 \tag{8}$$

where $\beta = T_0(3\lambda + 2\mu)/k$ and integration is carried out over the volume of the element. Similarly, substituting Eqs. (6) and (7) into Eq. (5) and using the weighting functions $\Phi_{mi}(x^s)$ gives

$$\sum_{m=1}^{n}\int_V \Big[\mu U_{mi}\phi_{mi,kk} + (\lambda + \mu)\, U_{mk}\phi_{mk,ki} - (3\lambda + 2\mu)\alpha\, T_m\,\Psi_{m,i} - \ell\ddot{U}_{mi}\phi_{mi}\Big]\phi_{li}\,\mathrm{d}V = 0$$

$$l = 1,n;\; i = 1,3 \tag{9}$$

Since the integration deals only with the spatial variables, the time functions $U_{mi}(t)$ and $T_m(t)$ and their time derivatives are removed from the integral and thus the two equations become

$$\sum_{m=1}^{n} T_m\int_V \Psi_{m,ii}\Psi_l\,\mathrm{d}V - \frac{1}{\kappa}\sum_{m=1}^{n}\dot{T}_m\int_V \Psi_m\,\Psi_l\,\mathrm{d}V - \beta\sum_{m=1}^{n}\dot{U}_{mi}\int_V \phi_{mi,i}\Psi_l\,\mathrm{d}V + \frac{Q}{k}\int_V \Psi_l\,\mathrm{d}V = 0$$

$$l = 1,n;\; i = 1,3 \tag{10}$$

$$\mu\sum_{m=1}^{n} U_{mi}\int_V \phi_{mi,kk}\phi_{li}\,\mathrm{d}V + (\lambda + \mu)\sum_{m=1}^{n} U_{mk}\int_V \phi_{mk,ki}\phi_{li}\cdot\mathrm{d}V - (3\lambda + 2\mu)\alpha\sum_{m=1}^{n} T_m\int_V \Psi_{m,i}\phi_{li}\,\mathrm{d}V - \ell\sum_{m=1}^{n}\ddot{U}_{mi}\int_V \phi_{mi}\,\phi_{li}\cdot\mathrm{d}V = 0 \tag{11}$$

These equations can be represented in matrix form and after assembly the final form of the equilibrium equations for coupled thermoelastic problems is

$$[A]\{T\} + [B]\{\dot{T}\} + [N]\{\dot{U}\} = \{q\} \tag{12}$$

$$[D]\{U\} + [E]\{T\} + [M]\{\ddot{U}\} = \{f\} \tag{13}$$

The initial and boundary conditions are the specified displacements and temperature at the boundary, $\{U\} = \{U_s\}$ and $\{T\} = \{T_s\}$.

The column matrices with a superposed dot represent the time derivative of that matrix, that is, $\{\dot{U}\} = (\mathrm{d}/\mathrm{d}t)\{U\}$. Taking the velocity matrix as $\{V\} = \{\dot{U}\}$, the final form for the equilibrium equation in terms of a combined matrix $\{X\}$ becomes

$$[C]\{\dot{x}\} + [K]\{x\} = \{F\} \tag{14}$$

where

$$\{x\} = \begin{Bmatrix}\{T\}\\ \{U\}\\ \{V\}\end{Bmatrix} \tag{15}$$

The matrices $[C]$ and $[K]$ are defined as

$$[C] = \left[\begin{array}{c|c|c}[B] & & \\ \hline & [I] & \\ \hline & & [M]\end{array}\right] \tag{16}$$

$$[K] = \left[\begin{array}{c|c|c}[A] & & [N] \\ \hline & & -[I] \\ \hline [E] & [D] & \end{array}\right] \tag{17}$$

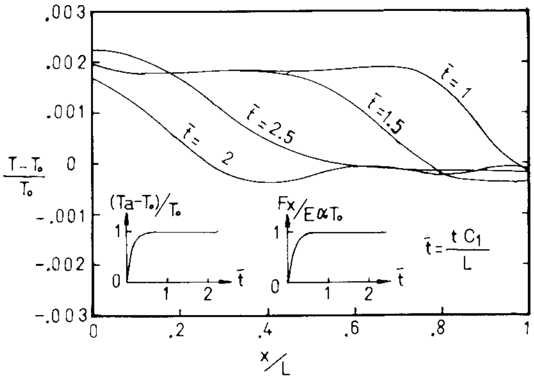

Fig. 1 Temperature vs axial distance at various times for both ends free beam.

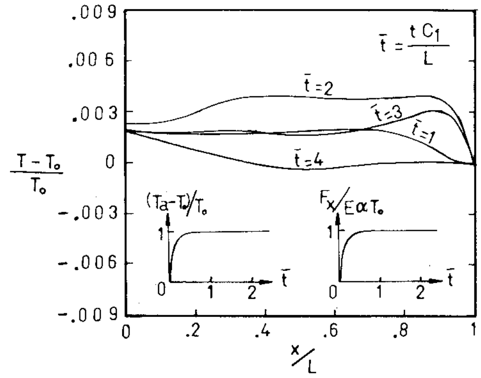

Fig. 3 Temperature vs axial distance at various times for cantilever beam.

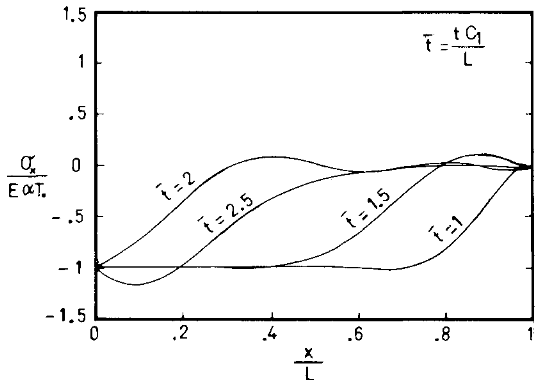

Fig. 2 Stress vs axial distance at various times for both ends free beam.

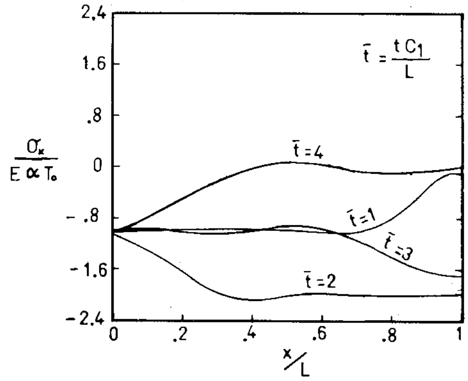

Fig. 4 Stress vs axial distance at various times for cantilever beam.

while the force matrix is

$$\{F\} = \begin{Bmatrix} \{q\} \\ \{f\} \\ \{O\} \end{Bmatrix} \tag{18}$$

This system of equations may be solved for the matrix $\{X\}$; stress and strain matrices are obtained easily afterward. The matrices $\{q\}$ and $\{f\}$ in the force matrix are related to the heat flow and the mechanical forces at the boundary of the solution domain, which are known from the initial and boundary conditions.

In order to discuss the method in more detail, a one-dimensional rod problem will be considered. The equilibrium equation in terms of the axial displacement is

$$E\frac{\partial^2 u}{\partial x^2} - E\alpha\frac{\partial T}{\partial x} = \ell\frac{\partial^2 u}{\partial t^2} \tag{19}$$

and the first law of thermodynamics reduces to

$$\frac{\partial^2 T}{\partial x^2} - \frac{1}{\kappa}\frac{\partial T}{\partial t} = \beta\frac{\partial^2 u}{\partial x \partial t} \tag{20}$$

Taking a line element of length L, the approximating function for the displacement is assumed to be linear in x as

$$u(x,t) = N_i U_i + N_j U_j = \langle N \rangle \{U\} \tag{21}$$

where the piecewise linear shape function $\langle N \rangle$ is $N_i = (L - X)/L$, $N_j = X/L$, and $X = x - x_i$. Similarly, the temperature is approximated by

$$T(x,t) = N_i T_i + N_j T_j = \langle N \rangle \{T\} \tag{22}$$

Applying the formal Galerkin method results in the equilibrium equation, Eq. (14), where the submatrices are

$$[A] = [D] = \int_0^l \begin{bmatrix} \dfrac{dN_i}{dx}\dfrac{dN_i}{dx} & \dfrac{dN_i}{dx}\dfrac{dN_j}{dx} \\ \dfrac{dN_j}{dx}\dfrac{dN_i}{dx} & \dfrac{dN_j}{dx}\dfrac{dN_j}{dx} \end{bmatrix} dx$$

$$[B] = \frac{1}{k}\int_0^l \begin{bmatrix} N_i N_i & N_i N_j \\ N_j N_i & N_j N_j \end{bmatrix} dx$$

$$[N] = \beta\int_0^l \begin{bmatrix} N_i\dfrac{dN_i}{dx} & N_i\dfrac{dN_j}{dx} \\ N_j\dfrac{dN_i}{dx} & N_j\dfrac{dN_j}{dx} \end{bmatrix} dx \tag{23}$$

The $[E]$ and $[M]$ matrices are

$$[E] = \frac{\alpha}{\beta}[N] + \begin{bmatrix} -1 & 0 \\ 0 & 1 \end{bmatrix}, \qquad [M] = \frac{k\ell}{E}[B] \tag{24}$$

and the force matrices are

$$\{q\} = \frac{1}{k}\begin{Bmatrix} q_i \\ -q_j \end{Bmatrix}, \qquad \{f\} = \frac{1}{E}\begin{Bmatrix} F_{x_i} \\ F_{x_j} \end{Bmatrix} \tag{25}$$

The components in the thermal force matrix $\{q\}$ are the gradients of temperature with respect to x, that is $q_i = k \cdot dT/dX$ at $x = x_i$ and is the applied or the calculated stress at node i.

Now, consider a beam of constant cross section with free-free boundary conditions. A means of support may be considered for the beam so that it stays free from any axial stress at the reference time. A thermal and mechanical shock will be applied to the left end of the beam. The thermal shock is assumed to be produced by a sudden change in the ambient temperature. This sudden temperature change is transformed to the beam by convection, resulting in a large thermal gradient at the exposed end. This case of loading is a realistic model of a shock wave formation. The variation of the temperature and axial stress along the beam is plotted for different times in Figs. 1 and 2. The same type of loading is imposed for a cantilever beam and the curves for the temperature and axial stress variation vs time are shown in Figs. 3 and 4. The main difference between the results is the value of the stress at the clamped vs free edges for two different types of beams. For the free-free beam, the axial stress at the end where the load is imposed varies, while at the opposite edge this variation of the axial stress is near zero. On the other hand, for the clamped beam where its free edge is exposed to the shock, the clamped edge experiences high variations of the axial stress. The case is quite relevant and shows the validity and power of the proposed method.

Conclusion

Problems of coupled thermoelasticity, while having a wide range of engineering applications, have not received a great deal of attention. The main reasons are complicated analytical solutions and the lack of a sound numerical method. Bahar and Hetnarski[5,6] have recently published a series of papers proposing the state-space approach. That method is, of course, sound for one-dimensional problems, but application to two- and three-dimensional problems seems to have some difficiencies. The method proposed in this Note, which is based on the Galerkin method, does not encounter any major deficiencies in its application to two- and three-dimensional problems and thus at present, seems to be the most appropriate finite-element formulation for this class of problems.

References

[1]Nowacki, W., *Thermoelasticity,* Pergamon, London, 1962.

[2]Fletcher, C. A. J., *Computational Galerkin Method,* Springer-Verlag, New York, 1984.

[3]Eslami, M. R. and Salehzadeh, A., "Application of Galerkin Method to Coupled Thermoelastic Problems," *5th International Modal Analysis Conference,* London, April 1987.

[4]Mitchell, A. R. and Watt, R., *The Finite Element in Partial Differential Equations,* Wiley, New York, 1978.

[5]Bahar, L. Y. and Hetnarski, R. B., "State-Space Approach to Thermoelasticity," *Journal of Thermal Stresses,* Vol. 1, No. 1, July 1978, pp. 135–146.

[6]Bahar, L. Y. and Hetnarski, R. B., "Direct Approach to Thermoelasticity," *Journal of Thermal Stresses,* Vol. 2, Jan. 1979, pp. 135–148.

Nonlinear Free Vibration of Elastic Plates

G. Chandrasekharappa* and H. R. Srirangarajan†
Indian Institute of Technology, Powai, Bombay, India

Introduction

THE effect of large deflection on the free nonlinear vibrations of elastic plates, based on von Kármán's large deflection plate theory, has been considered by many researchers. By applying Herrmann's theory, Chu and Herrmann[1] studied the influence of large deflections on the free vibrations of a rectangular plate with hinged immovable edges. By using the first-order approximation to that of Herrmann, Yamaki[2] investigated one-term solutions for simply supported and clamped plates for free and forced sinusoidal vibrations. Using the perturbation method of Poincare's as modified by Lighthill, Bauer[3] investigated the flexural vibrations of plates with simply supported and clamped boundary conditions, subjected to the step function and the exponentially decaying pulse. The influence of initial membrane stress on the free and forced nonlinear vibration of beams and rectangular plates was investigated by Eisley[4] by means of a simple extension of the results for the unstressed case by using single-mode representation.

In this paper, the influence of large amplitudes on free vibrations of square and circular plates for simply supported and clamped-in boundary conditions and for immovably constrained and stress-free edge conditions are studied by applying Anderson's[5,6] ultraspherical polynomial approximation (UPA) technique for solving the nonlinear differential equation in time. The results of the UPA technique are compared with the elliptic function method (EFM).

Received July 16, 1986; revision received Jan. 13, 1987.

*Research Scholar, Department of Mechanical Engineering.
†Assistant Professor, Department of Mechanical Engineering.

Square Plates

The dynamic von Kármán equations for the free vibration of plates may be written as

$$\nabla^4 F = E\left[\left(\frac{\partial^2 W}{\partial x \partial y}\right)^2 - \left(\frac{\partial^2 W}{\partial x^2}\right)\left(\frac{\partial^2 W}{\partial y^2}\right)\right] \tag{1}$$

$$L(W,F) = D\nabla^4 W + \rho h \frac{\partial^2 W}{\partial t^2} - h\left[\frac{\partial^2 F}{\partial y^2}\frac{\partial^2 W}{\partial x^2} + \frac{\partial^2 F}{\partial x^2}\frac{\partial^2 W}{\partial y^2} - 2\frac{\partial^2 F}{\partial x \partial y}\frac{\partial^2 W}{\partial x \partial y}\right] = 0 \tag{2}$$

In these equations, the effects of both the longitudinal and rotatory inertia forces have been neglected and correspond to the first approximation to those of Herrmann as stated by Chu and Herrmann.[1] The boundary conditions considered are the simply supported (SS) and the clamped-in (CI); and the edge conditions considered are the stress-free (SF) and the immovably constrained (IC).[3] The solution for a simply supported square plate is assumed to be

$$W(x,y,t) = hf(t)\cos(\pi x/a)\cos(\pi y/a)$$

Airy's stress function is expressed as

$$F(x,y,t) = F^*(x,y)f^2(t)$$

Following Bauer's[3] procedure, we get, for the SF case,

$$\ddot{f}(t) + \omega^2 f(t) + \epsilon\omega^2 f^3(t) = 0 \tag{3}$$

where

$$\omega^2 = \frac{\pi^4 E h^2}{3\rho(1-\nu^2)a^4}$$

$$\epsilon = 0.19476(1-\nu^2)$$

A similar procedure is followed in other cases, and the resulting equation is of the form of Eq. (3). The values ω^2 and ϵ in each case are given in Table 1.

Circular Plates

The dynamic von Kármán equations for the free vibration of circular plates are written as

$$\nabla^4 F = -\frac{E}{r}\frac{\partial W}{\partial r}\frac{\partial^2 W}{\partial r^2} \tag{4}$$